JOURNAL OF MATERIALS SCIENCE 24 (1989) 1867–1880

Preparation and sintering of narrow-sized Al_2O_3–TiO_2 composite powders

HIROMICHI OKAMURA*, ERIC A. BARRINGER‡, H. KENT BOWEN
Ceramics Processing Research Laboratory, Materials Processing Center, Massachusetts Institute of Technology, Cambridge, Massachusetts 02139, USA

Narrow size distribution Al_2O_3–TiO_2 composite powders containing nominally 10 to 60 mol% TiO_2 were prepared by the stepwise hydrolysis of titanium alkoxide in an Al_2O_3 dispersion. Particle size was controlled by selecting the particle size of the starting Al_2O_3 powder. The TiO_2 content was determined by the amount of alkoxide hydrolysed. Composite powder compacts were prepared by filter casting or centrifugal casting the composite powder dispersions. All compacts had similar shrinkage behaviour during sintering. When fired above 1300° C, the compacts containing less than 50 mol% TiO_2 became Al_2TiO_5–Al_2O_3 composite bodies with high densities, the compact containing 50 mol% TiO_2 became an Al_2TiO_5 body with domain structure, and the compact containing 60 mol% TiO_2 formed a TiO_2–Al_2TiO_5 composite structure. When these composite bodies were annealed below 1300° C, they showed different decomposition behaviour and microstructures.

1. Introduction

To obtain high-quality, reliable, ceramic materials, the macro- and microstructure of the ceramic body must be controlled during fabrication [1]. The microstructure, which develops during sintering, is largely determined by powder characteristics (e.g. particle size, size distribution, shape, state of agglomeration, and chemical composition) and particle packing in the green body [1, 2].

Ceramic composite powders are ordinarily prepared by conventional processing methods such as ball-milling and isostatic pressing. Such methods, however, often do not yield powders mixed homogeneously on a microscopic scale, and do not allow control of particle size and shape. Therefore, a synthesis technique utilizing a coating procedure was studied to produce composite powders with a homogeneous chemical composition and a narrow size distribution.

This synthesis technique has several advantages that make it attractive for producing ceramic composite powders. For example, the chemical composition of each particle can be controlled by selecting the starting powder, the coating material, and the quantitative ratio of the two. Also, the particle size of the final coated powder can be controlled by selecting the starting Al_2O_3 powder's particle size and by adjusting the amount of coating. (However, changing the amount of coating for a given Al_2O_3 particle size changes the final composition.) Furthermore, this process is easily adaptable to continuous processing schemes [3–6], multicomponent, narrow-sized powders can be prepared, and the basic technique might be applied to other systems, such as Al_2O_3–ZrO_2 and Al_2O_3–SiO_2.

This report describes the preparation, characterization, processing, and sintering of narrow-sized TiO_2-coated Al_2O_3 powders. Microstructures for sintered and for sintered and annealed compacts were also studied. The results demonstrate that these powders can be sintered to Al_2O_3–TiO_2, Al_2TiO_5–Al_2O_3, Al_2TiO_5, or Al_2TiO_5–TiO_2 composite ceramics, depending on the sintering temperature and the chemical composition of the TiO_2-coated Al_2O_3 powders. A preliminary report of this research was presented at the Second International Conference on Ultrastructure Processing of Ceramics, Glasses and Composites [7].

2. Experimental procedure

2.1. Preparation of TiO_2-coated Al_2O_3 powders

TiO_2-coated Al_2O_3 powders containing 10 to 60 mol% TiO_2 were prepared by the stepwise controlled hydrolysis of titanium tetraisopropoxide, $Ti(OC_3H_7^i)_4$, in a dispersion of Al_2O_3 in isopropyl alcohol. The starting material used to prepare the Al_2O_3–TiO_2 samples was high-purity Al_2O_3 with a narrow particle-size distribution (mean particle diameter = 0.2 to 0.3 μm; standard deviation = 30% of the mean), prepared from a dispersion of commercial powder (Alcoa XA-139 S.G., Pittsburgh, Pennsylvania, USA) by centrifugal separation into particle size classifications [8].

In the experiment reported here, a 0.06 M solution

Present address: Nippon Soda Co. Ltd, Japan.
‡*Present address*: Ceramics Process Systems, Inc., Cambridge, Massachusetts, USA.

0022–2461/89 $03.00 + .12

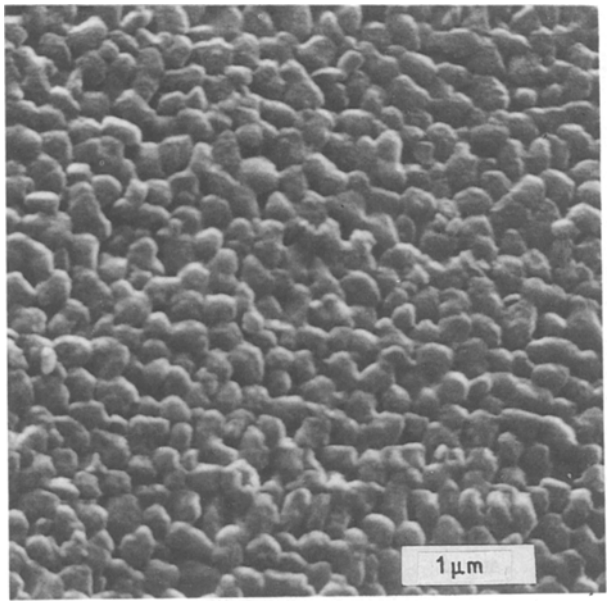

Figure 1 Scanning electron micrograph of the top surface of an Al_2O_3–50 mol % TiO_2 green compact made by centrifugal casting. (Figs 1, 2, 7, 9, 10, 11a, 12, and 13 are reprinted with permission from *J. Amer. Ceram. Soc.* [15])

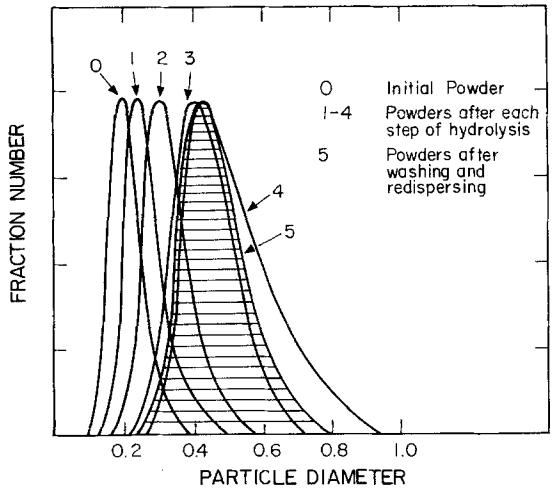

Figure 2 Particle size distributions of the initial and composite (50 mol % TiO_2) powders after each hydrolysis reaction step, and of the composite powder after washing and redispersion.

of Al_2O_3 in isopropyl alcohol (6.1 g Al_2O_3/litre alcohol) was prepared by ultrasonically dispersing the Al_2O_3 (dried at 140° C for 24 h) in dry isopropyl alcohol (refluxed with CaH_2, then distilled). A 0.12 M solution of $Ti(OC_3H_7^i)_4$ (Alpha Products, Danvers, Massachusetts, USA) in isopropyl alcohol, and a 2.4 M solution of water in isopropyl alcohol, were prepared separately. To prepare Al_2O_3–TiO_2 composite samples containing 10, 20, 30, 40, 50, or 60 mol % TiO_2, different volumes of the alkoxide and water solutions were added to the Al_2O_3 solution. These volumes were increased nominally from one-eighteenth to one-eighth, three-fourteenths, one-third, one-half, and three-fourths of the Al_2O_3 dispersion's volume, respectively.

To avoid serious agglomeration of the coated powder during hydrolysis, the solutions of alkoxide and water were added stepwise to the Al_2O_3 dispersion. The number of steps for hydrolysis was determined so that the amount of alkoxide hydrolysed per step could be kept at a level less than 15 mol % of the amount of dispersed Al_2O_3 powder; at higher levels, the coating procedure produced highly agglomerated powders. Therefore, a 50 mol % TiO_2 coating was achieved in four steps, 30 mol % TiO_2 in three steps, and so on. For comparison, an Al_2O_3–50 mol % TiO_2 composite powder was prepared using a single-step procedure in which both the water and the alkoxide solution were added all at once to the Al_2O_3 dispersion.

Before the stepwise hydrolysis reaction, water in the amount of five times the molar ratio to Al_2O_3 was added to the Al_2O_3 dispersion, which was being stirred, to saturate partially the Al_2O_3 powder surface with adsorbed water. Without this procedure, it was found that the alkoxide's first hydrolysis reaction was extremely slow, because dried Al_2O_3 powders adsorb water so strongly that the free water concentration was reduced below the necessary level (less than 3 molar ratio of water to alkoxide).

Each step of the hydrolysis reaction was performed by adding one portion of water solution first, then one portion of alkoxide solution to the Al_2O_3 dispersion,

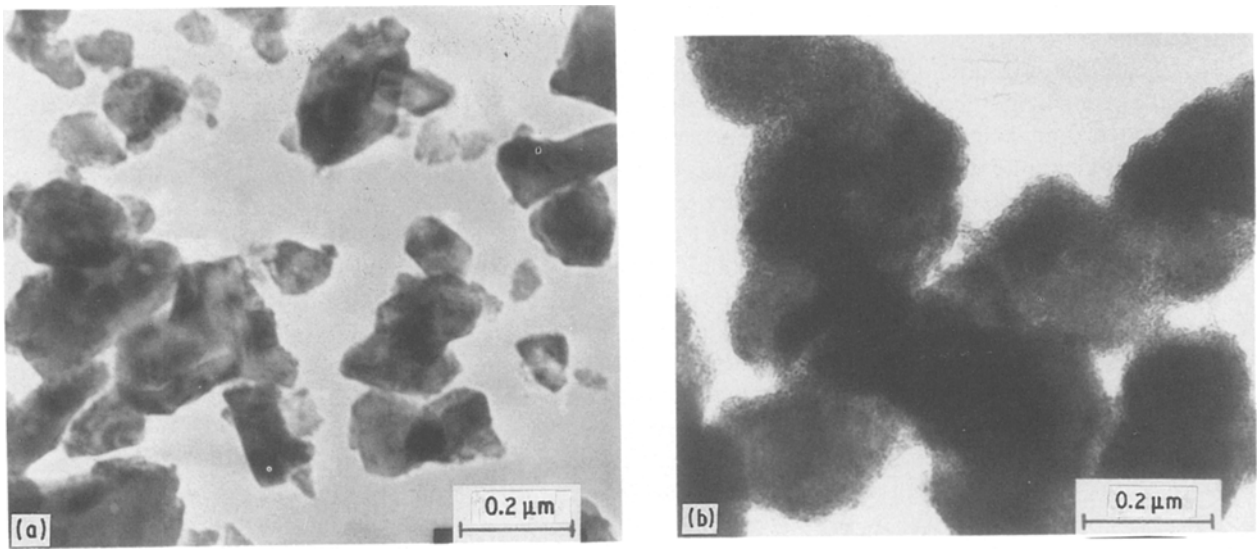

Figure 3 Transmission electron micrograph of (a) the starting α-Al_2O_3 powder, and (b) the TiO_2-coated Al_2O_3 powder (30 mol % TiO_2).

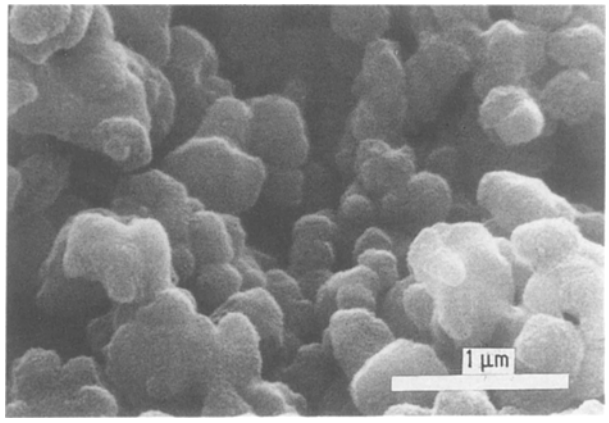

Figure 4 Scanning electron micrograph of an Al_2O_3–50 mol % TiO_2 powder made by the single-step hydrolysis of $Ti(OR)_4$.

and stirring by magnetic stirrer for 15 min. After each hydrolysis step, the solution was redispersed (using an ultrasonic bath) to measure powder particle size and distribution using a photon correlation particle analyser (Coulter Electronics Inc. N-4 Submicron Particle Analyzer, Hialeah, Florida, USA). After confirming that the powder was adequately redispersed, the next hydrolysis step was performed.

The dispersion of coated powder was centrifuged to remove the alcohol solution, then washed with deionized water and ultrasonically redispersed in a dilute aqueous solution of NH_4OH (pH 10). This dispersion was stocked in a plastic bottle. The final coated and washed powder particle size and distribution were measured using the photon correlation particle analyser.

2.2. Characterization of the composite powders

Scanning electron microscopy (SEM) and transmission electron microscopy (TEM) were used to estimate particle size and morphology. Quantitative size distributions were measured by photon correlation spectroscopy using the Coulter Model N-4D. Specific surface areas of the powders were measured by nitrogen gas adsorption (single-point BET method) (Quantasorb, Quantachrom Corp., Syosset, New York, USA). Powder densities were measured using a stereopycnometer (Quantachrom Corp.) and helium gas. Crystallinity was determined by powder X-ray diffraction using Cu$K\alpha$ radiation. Differential thermal analysis (DTA) and thermogravimetric analysis (TGA) (Netzch Corp., Exton, Pennsylvania) were done in air at a heating rate of $10°C\,min^{-1}$. The chemical composition of the composite powders was determined by quantitative X-ray diffraction analysis, performed after calcination at 1000° C for 3 h.

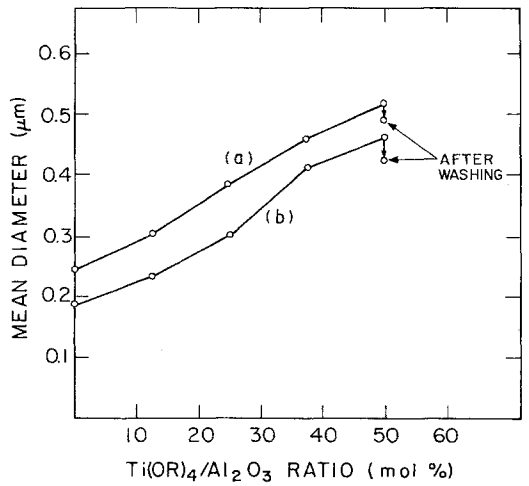

Figure 5 Mean diameter changes of particles after each hydrolysis step for two different batches that used Al_2O_3 powders having mean diameters of (a) 0.25 μm, and (b) 0.19 μm.

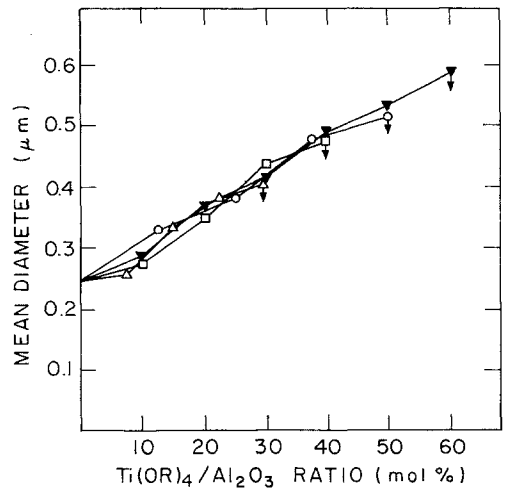

Figure 6 Mean diameter of particles after each hydrolysis step for four different batches in which the total amount of alkoxide was changed from 30 to 60 mol %. (△) 30 mol % $Ti(OR)_4$, (□) 40 mol % $Ti(OR)_4$, (○) 50 mol % $Ti(OR)_4$, (▼) 60 mol % $Ti(OR)_4$.

2.3. Sintering of the composite powders

Composite powder compacts were prepared by centrifugal casting or filter casting from the composite powder dispersions. Green compacts were air dried at room temperature and then dried at 140° C for 24 h. Before firing, compacts were calcined in air at 450° C for 1 h to remove organic material.

Some of the 50 mol % TiO_2 compacts were fired in air at a temperature below 1300° C; others were fired at a temperature above 1300° C for time periods ranging from 30 to 20 h. Compacts with TiO_2 contents of 10, 20, 30, 40, and 60 mol % were fired at 1500° C for 30 min to 9 h. The shrinkage behaviour during firing was observed with a dilatometer (Netzsch Corp., Exton, Pennsylvania, USA). After sintering, some compacts were annealed at 1200° C; others were

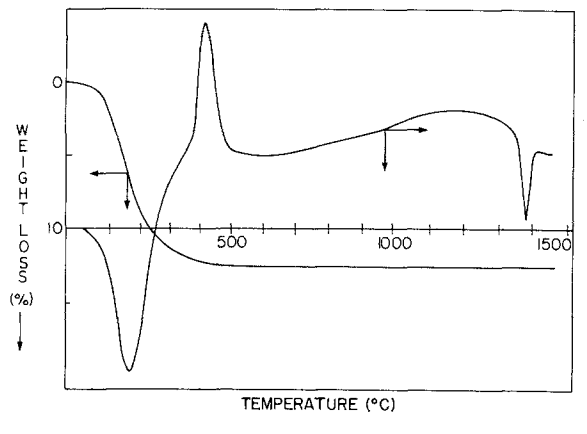

Figure 7 DTA and TGA curves for Al_2O_3–50 mol % TiO_2 powders.

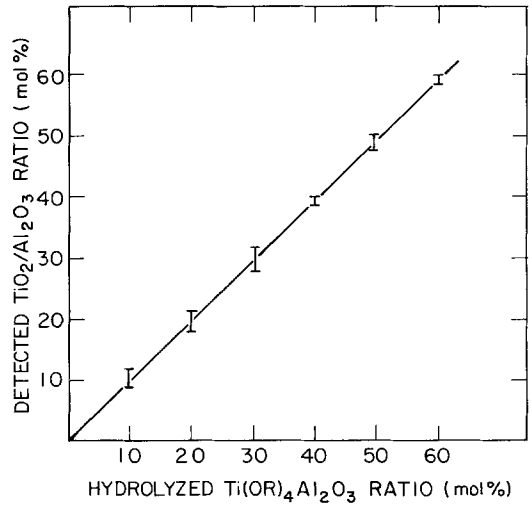

Figure 8 Detected TiO_2 content plotted against hydrolyzed $Ti(OR)_4$ content. All powders were calcined at 1000° C for 3 h before X-ray diffraction analysis.

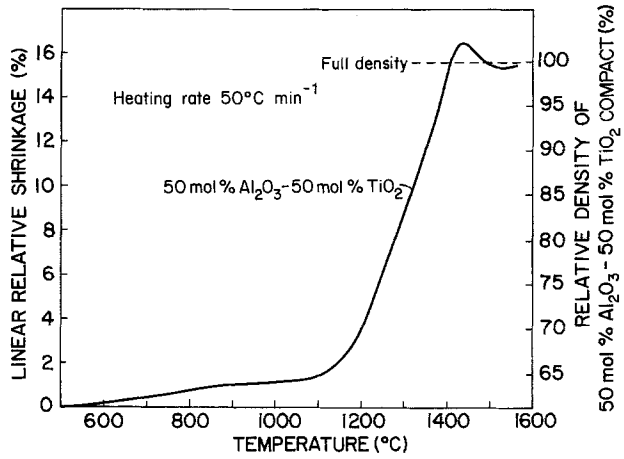

Figure 9 Sintering behaviour of Al_2O_3–TiO_2 compacted powder fired in air at a rate of 50° C min^{-1}.

cooled to 200° C then annealed at 1200° C for 30 min to 16 h.

2.4. Microstructure and physical properties of the fired compacts

Microstructures of the sintered and of the sintered and annealed compacts were examined by SEM and optical microscopy. The densities of the fired compacts were measured by the Archimedes method. The chemical composition of each compact was analysed by electron probe microanalysis using well-characterized standards. Fracture toughness (K_{Ic}) of the fired bodies was determined by the microindentation test using a micro-Vickers hardness tester. The specimens were polished, or polished and chemically etched for SEM backscattering image analysis and optical microscopic analysis using polarized light reflection.

3. Results and discussion

3.1. Characterization of the synthesized powder

The unagglomerated, narrow-sized Al_2O_3–50 mol % TiO_2 composite powder (Al_2O_3/TiO_2 = 1) synthesized is shown in Fig. 1. Composite particle growth during the stepwise hydrolysis reaction as measured by the photon correlation particle analyser is shown in Fig. 2. TEM demonstrated that the composite powder with 30 mol % TiO_2 was composed of α-alumina crystals coated with amorphous TiO_2 (Figs 3a, b). These desirable powder characteristics were maintained in all the composite powders having different TiO_2 contents.

When the single-step coating was used instead of the stepwise coating, highly agglomerated powder was obtained, as shown in Fig. 4. These results show the useful effect of the stepwise coating process to produce unagglomerated powders. The reproducibility of this process is illustrated in Figs 5 and 6. In two different batches that used Al_2O_3 powders with different mean diameters, and in four different batches in which the total amount of alkoxide was changed from 30 to 60 mol %, the mean diameter of particles after each hydrolysis step increased at almost the same rate. Thus, the size of the coated powder could be controlled by selecting the size of the starting powder.

Table I summarizes the physical properties measured for composite powders containing nominally 10, 20, 30, 40, 50 and 60 mol % TiO_2. The TiO_2-coated

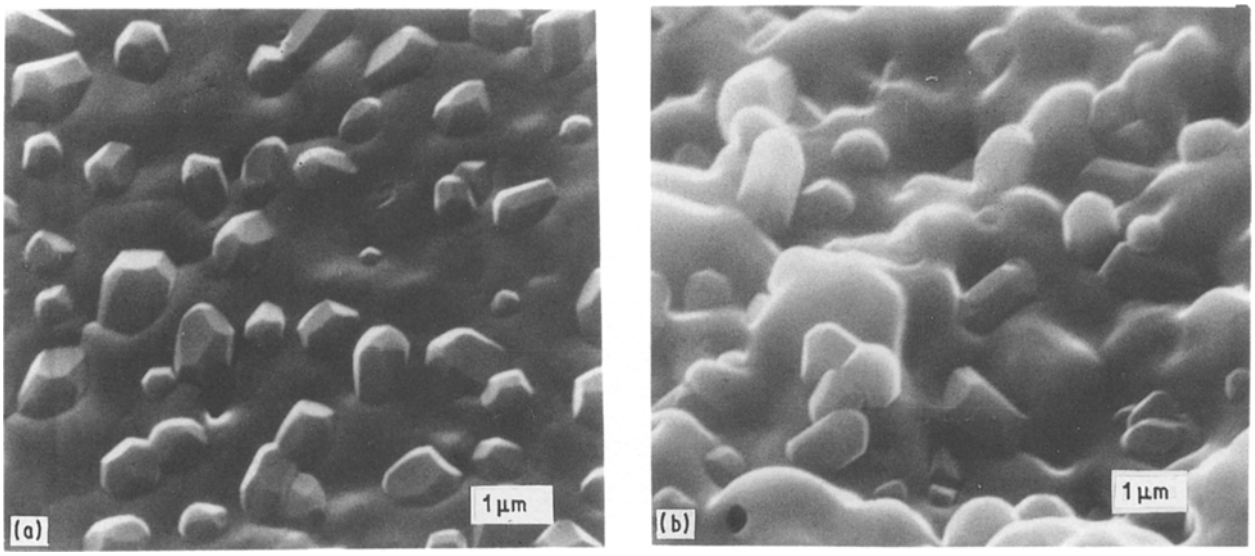

Figure 10 Scanning electron micrographs of an Al_2O_3–50 mol % TiO_2 compact fired at 1350° C for 30 min: (a) top surface, and (b) fracture surface.

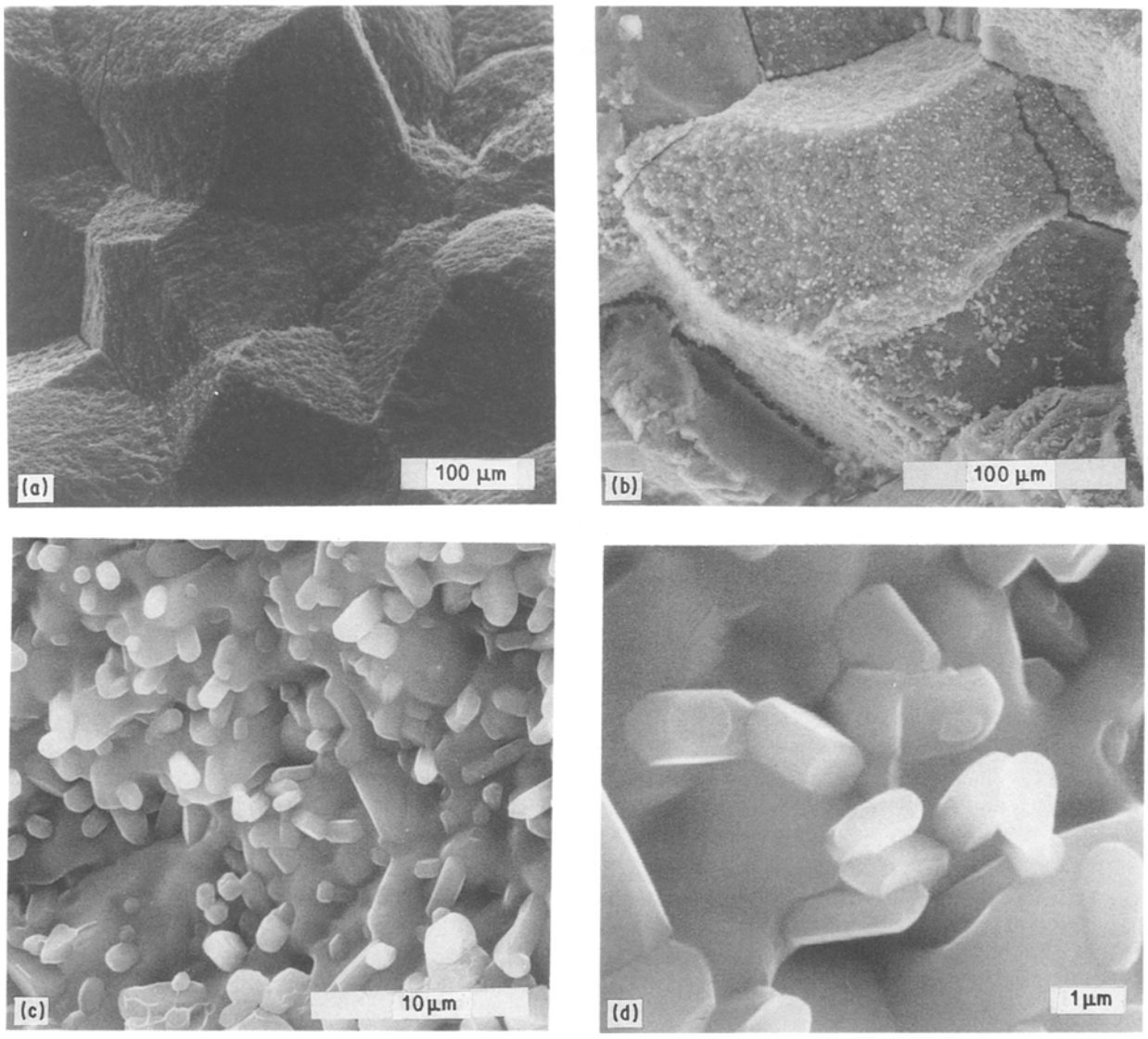

Figure 11 Scanning electron micrographs of the top surface of an Al_2O_3–50 mol % TiO_2 compact fired at 1350° C for 30 min, showing domain structure.

powders consisted of spheroidal particles having a narrow size distribution and a large surface area (190 to 210 $m^2 g^{-1}$ for the 50 mol % TiO_2 compact). X-ray diffraction showed the TiO_2 coating phase to be amorphous for all powders. As mentioned previously, particle size increased with the amount of TiO_2 coating, but particle shape and structure was not affected. Density measurements obtained with a steropycnometer gave values inversely proportional to the TiO_2 level.

The results of simultaneous DTA–TGA analyses conducted on Al_2O_3–50 mol % TiO_2 powders are given in Fig. 7. Most weight loss was due to water loss between 90 and 250° C; the remainder resulted from burn-off of organics between 370 and 480° C. The DTA curve shows an endothermic peak in the temperature range where water was lost, and an exothermic peak in the region where organics were burned off. Another endothermic peak was observed between

TABLE I Physical properties of TiO_2-coated Al_2O_3 powders

Powder*	Precursor	Crystal form	Average particle characteristics				
			Size range (μm)	Density ($g cm^{-3}$)	Surface area ($m^2 g^{-1}$)	Shape	Structure
Initial		Al_2O_3	0.2–0.3	3.9	10–15	Irregular polyhedral (angular)	Singlet
10 mol % TiO_2	$Ti(OPr^i)_4$	Amorphous + Al_2O_3	0.2–0.3	3.8	20–30	Rounded	Singlet
20 mol % TiO_2	$Ti(OPr^i)_4$	Amorphous + Al_2O_3	0.3–0.4	3.7	25–30	Rounded	Singlet
30 mol % TiO_2	$Ti(OPr^i)_4$	Amorphous + Al_2O_3	0.3–0.4	3.7	35–45	Rounded	Singlet
40 mol % TiO_2	$Ti(OPr^i)_4$	Amorphous + Al_2O_3	0.4–0.5	3.6	110–120	Rounded	Singlet
50 mol % TiO_2	$Ti(OPr^i)_4$	Amorphous + Al_2O_3	0.4–0.6	3.5	190–210	Rounded	Mostly singlet
60 mol % TiO_2	$Ti(OPr^i)_4$	Amorphous + Al_2O_3	0.5–0.7	3.4	240–260	Rounded	Mostly singlet

*Washed with deionized water.

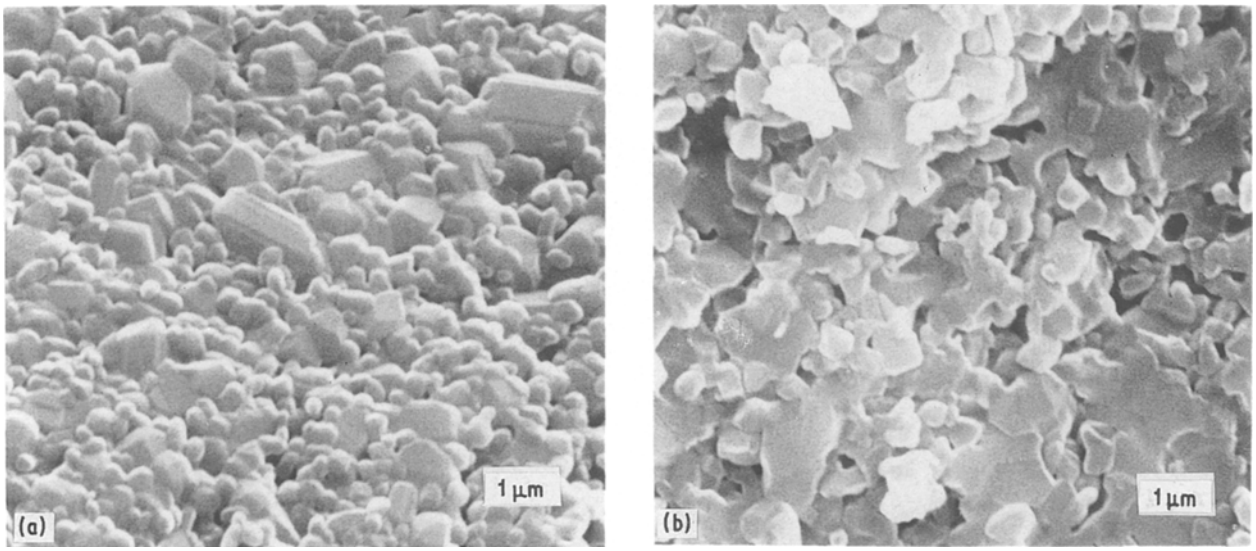

Figure 12 Scanning electron micrographs of an Al_2O_3–50 mol % TiO_2 compact fired at 1280° C for 4.5 h. (a) top surface, and (b) fracture surface.

1350 and 1410° C; this is assumed to be due to Al_2TiO_5 formation.

X-ray diffraction analyses were made for the Al_2O_3–50 mol % TiO_2 powder calcined under different conditions. The results are given in Table II. The TiO_2 crystal phase changed from amorphous to anatase, then to rutile, and finally to Al_2TiO_5 with the increasing temperature of calcination. The formation reaction of Al_2TiO_5 occurred above 1320° C, as expected from the DTA results; this temperature is higher than would be expected from the phase diagram [9].

Fig. 8 shows the results of quantitative X-ray diffraction analyses for the TiO_2 content of the coated powders. The amounts of TiO_2 detected were directly proportional to the amounts of alkoxide hydrolysed. The conversion factor of $Ti(OR)_4$ to TiO_2 was approximately 0.98.

3.2. Microstructure of the fired composite powder compacts

The Al_2O_3–50 mol % TiO_2 compacts (55% bulk density) were fired in air at a constant heating rate of 50° C min^{-1}. The linear relative shrinkage of the compacts during firing is given in Fig. 9. Shrinkage at the lower temperatures (below 1000° C) is due to the phase changes (amorphous → anatase → rutile) undergone by the coating. Shrinkage between 1100 and 1300° C is due to the densification of the rutile. Shrinkage between 1300 and 1400° C is due to the densification of the rutile phase combined with Al_2TiO_5 formation. At the temperature region above 1400° C, where Al_2TiO_5 phase formation becomes dominant, the sample expanded because Al_2TiO_5 has a slightly lower density than does an equivalent mixture of Al_2O_3 and rutile.

The Al_2O_3–50 mol % TiO_2 compacts fired at 1350° C for 30 min formed 100% Al_2TiO_5, and had relative densities of 95 to 99% (Fig. 10). The 1350° C/30 min firing schedule resulted in crystallographic domain formation (Fig. 11); cracks formed between domains due to anisotropic thermal contraction and large domain size. In a domain, Al_2TiO_5 crystals have almost the same orientation.

Compacts fired at 1280° C for 4.5 h had a two-phase

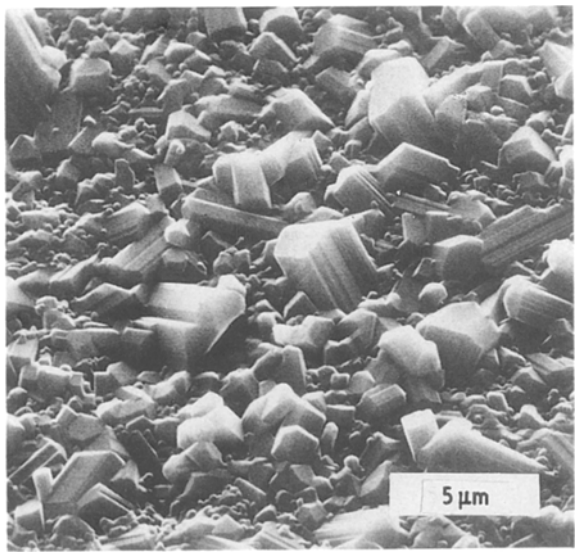

Figure 13 Scanning electron micrograph of the top surface of an Al_2O_3–50 mol % TiO_2 compact fired at 1280° C for 20 h.

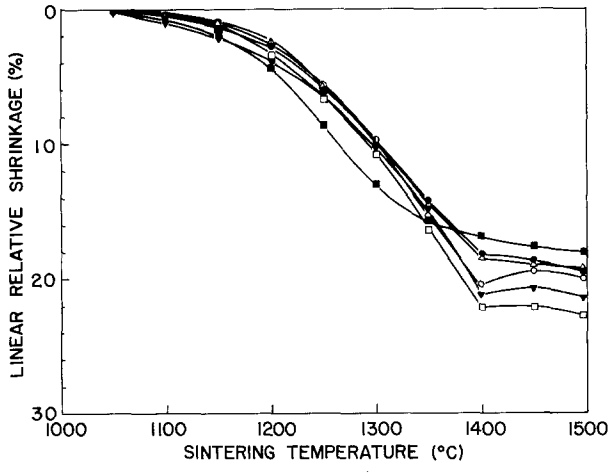

Figure 14 Sintering behaviour for Al_2O_3–TiO_2 compacted powders containing 10 to 60 mol % TiO_2 and fired in air at a rate of 50° C min^{-1}. TiO_2(mol %): (■) 10, (●) 20, (△) 30, (□) 40, (○) 50, (▼) 60.

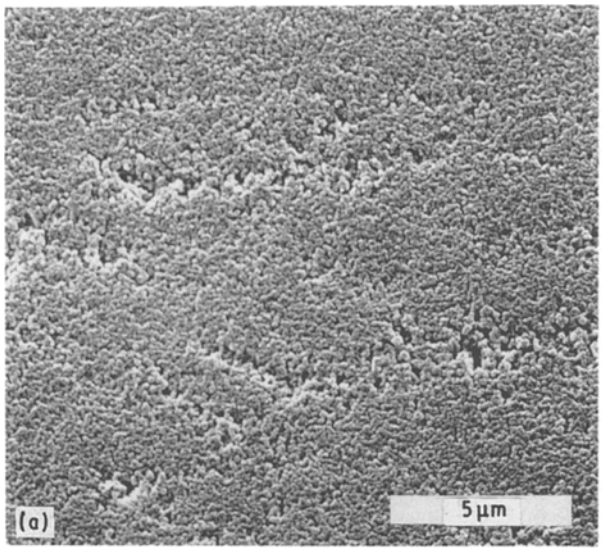

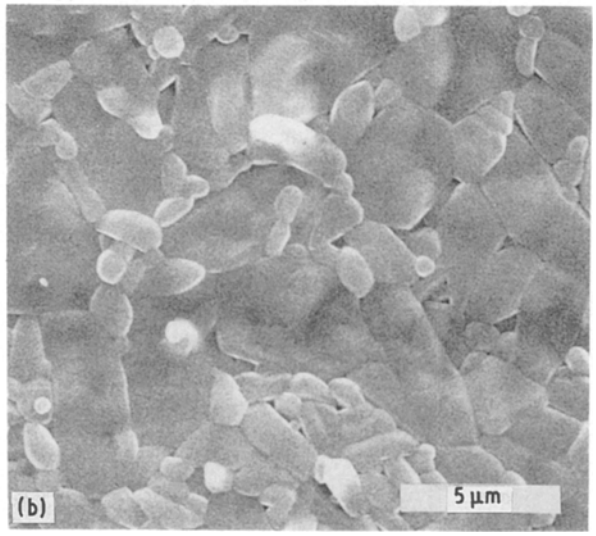

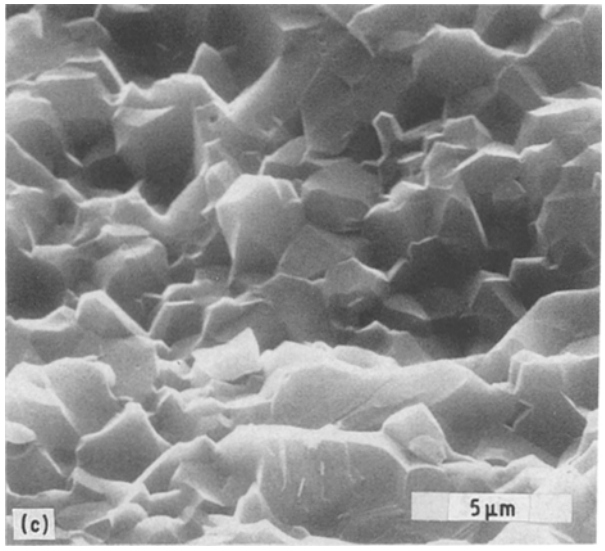

Figure 15 Scanning electron micrographs of: (a) the top surface of an Al_2O_3–10 mol % TiO_2 green compact made by filter casting, (b) the top surface of the same compact fired at 1500° C for 30 min, and (c) a fracture surface of the fired compact.

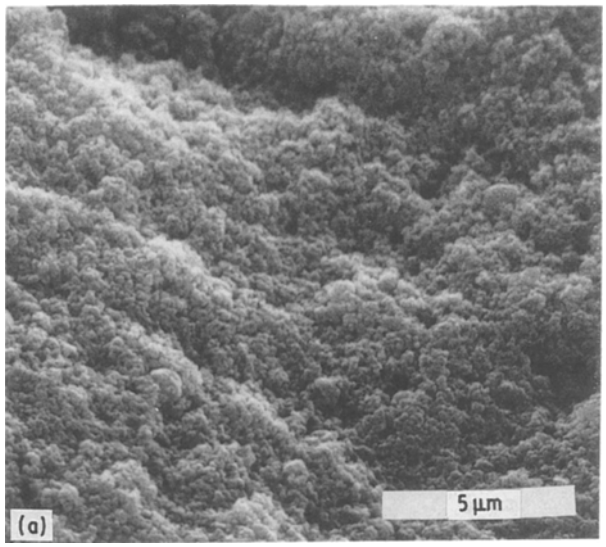

Figure 16 Scanning electron micrographs of: (a) the top surface of an Al_2O_3–20 mol % TiO_2 green compact made by filter casting, (b) the top surface of the same compact fired at 1500° C for 30 min, and (c) a fracture surface of the fired compact.

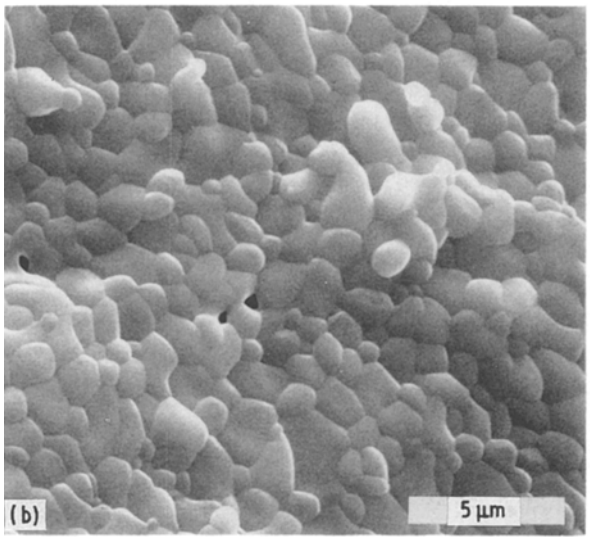

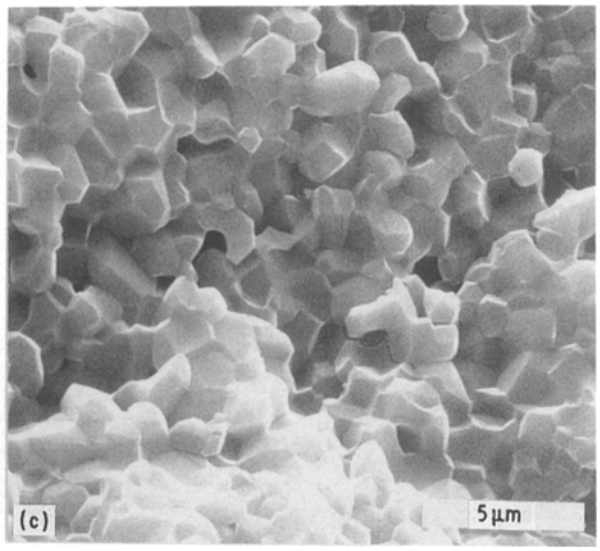

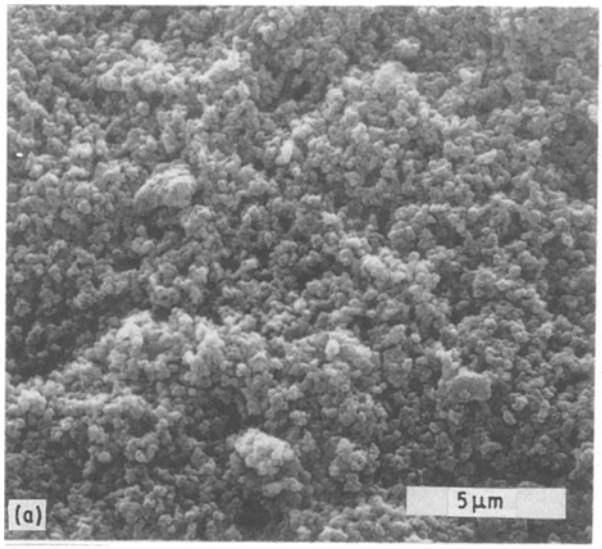

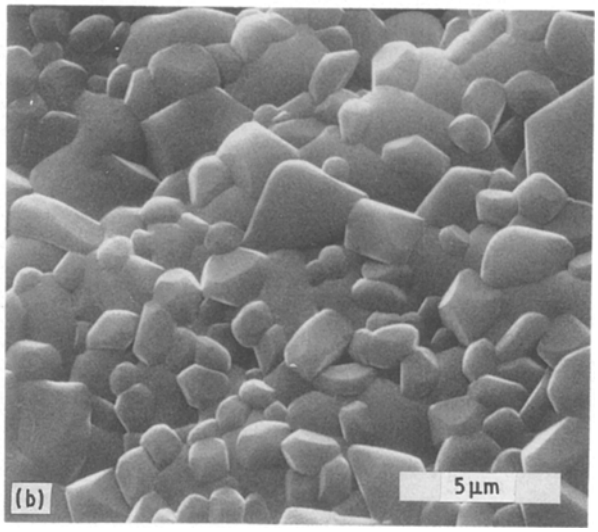

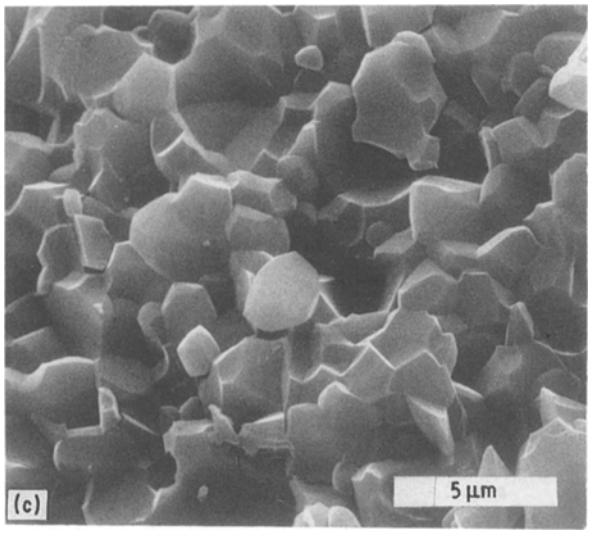

Figure 17 Scanning electron micrographs of: (a) the top surface of an Al_2O_3–30 mol % TiO_2 green compact made by filter casting, (b) the top surface of the same compact fired at 1500° C for 5 h, and (c) a fracture surface of the fired compact.

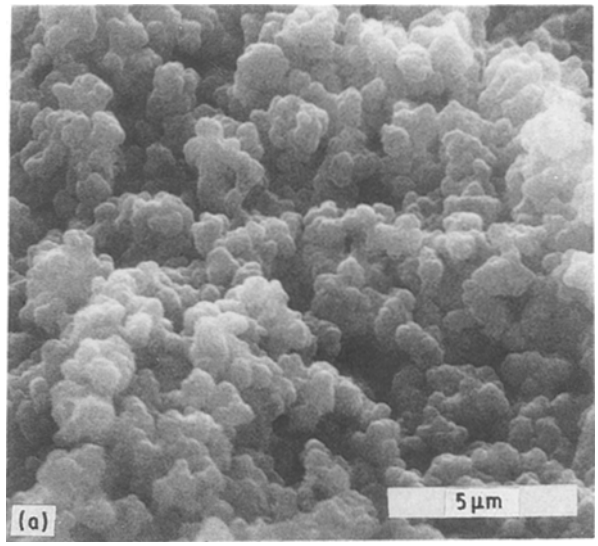

Figure 18 Scanning electron micrographs of: (a) the top surface of an Al_2O_3–60 mol % TiO_2 green compact made by filter casting, (b) the top surface of the same compact fired at 1500° C for 5 h, and (c) a fracture surface of the fired compact.

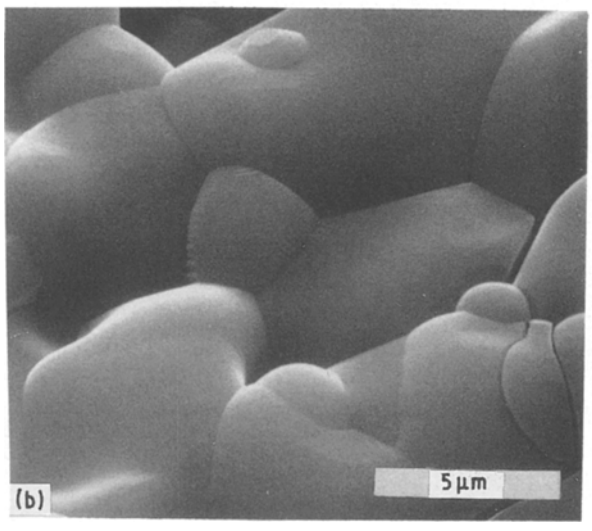

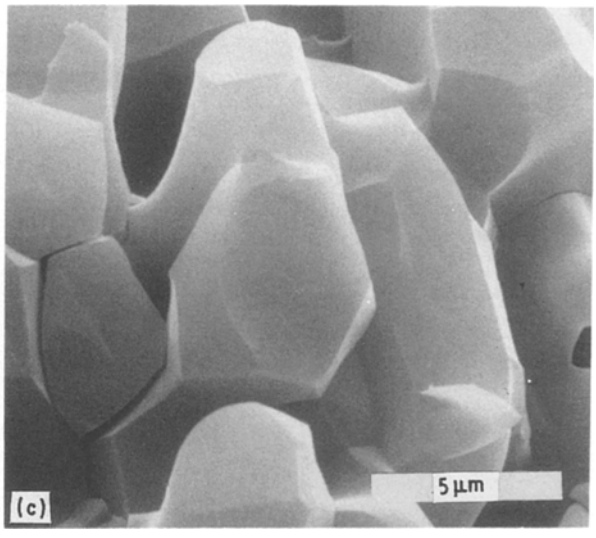

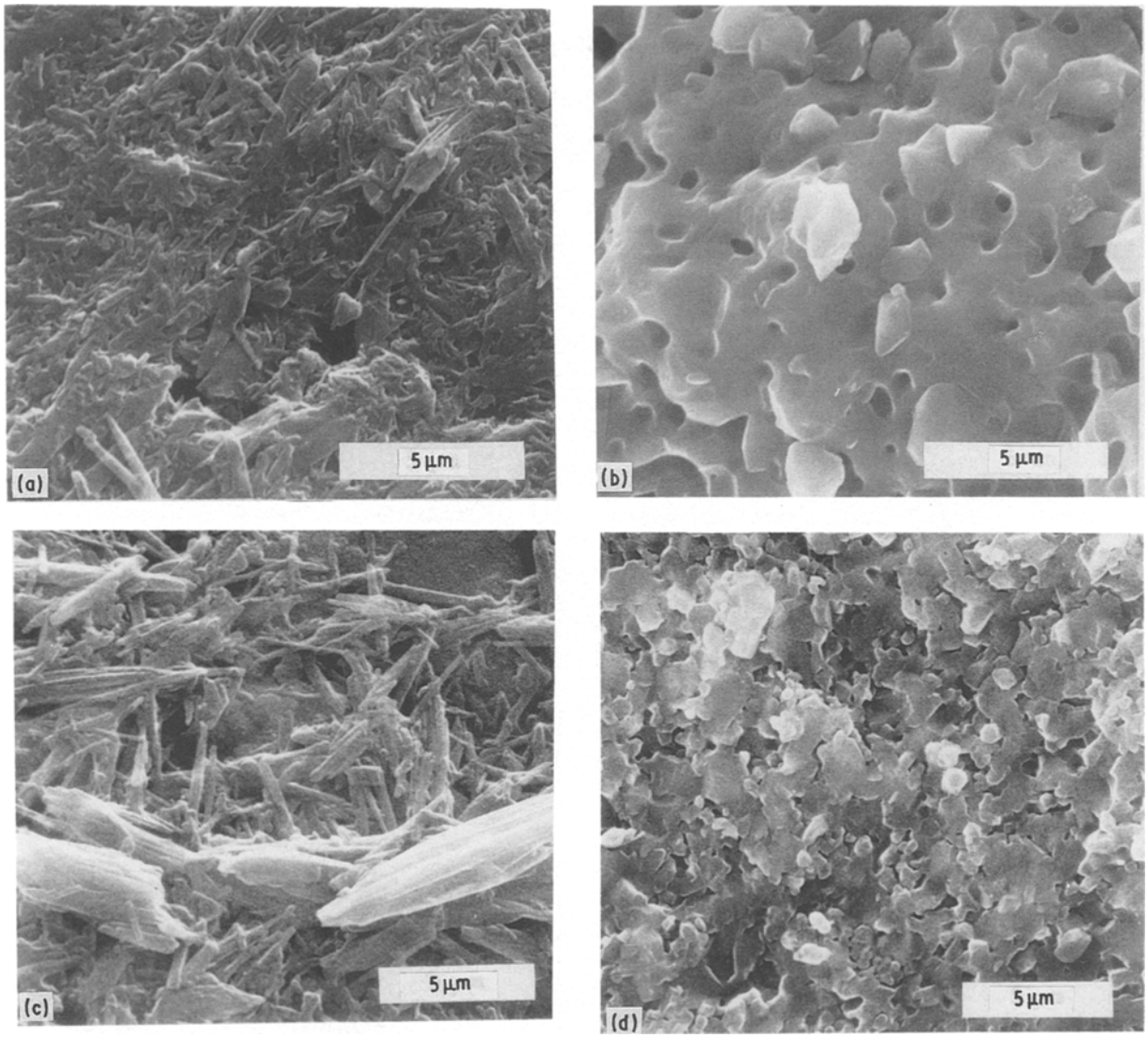

Figure 19 Scanning electron micrographs of: (a) polished and chemically etched surface, and (b) fracture surface of an Al_2O_3–50 mol % TiO_2 compact fired at 1350° C for 5 h; (c) polished and chemically etched surface, and (d) fracture surface of the same composition compact fired at 1280° C for 20 h.

structure of rutile and Al_2O_3 and were 85% theoretical density (Fig. 12); prolonged heating (1280° C, 20 h) increased the density to 90% theoretical and promoted rutile crystal growth, as shown in Fig. 13. No domain structure was observed in this specimen sintered at low temperature. These results indicate that Al_2TiO_5 formation occurs above 1300° C, as expected from the endothermic peak found in the differential thermal analysis results (Fig. 7).

TABLE II X-ray diffraction results for calcined Al_2O_3–50 mol % TiO_2 powders

Calcining conditions		Crystal form	
(° C)	(h)	TiO_2	Al_2O_3
140	5	Amorphous	Al_2O_3
500	3	Anatase	Al_2O_3
1000	3	Rutile	Al_2O_3
1280	5	Rutile	Al_2O_3
1280	20	Rutile	Al_2O_3
1300	2	Rutile	Al_2O_3
1320	2	Rutile + Al_2TiO_5	Al_2O_3 + Al_2TiO_5
1350	0.5	Al_2TiO_5	Al_2TiO_5
1400	0.5	Al_2TiO_5	Al_2TiO_5

Other compacts having different TiO_2 contents (10, 20, 30, 40 and 60 mol %) showed similar linear relative shrinkage, as shown in Fig. 14. However, the expansion at 1400° C caused by Al_2TiO_5 formation became smaller for the compacts having lower TiO_2 contents, and a higher sintering temperature (1500° C) was necessary to achieve densities greater than 95% theoretical.

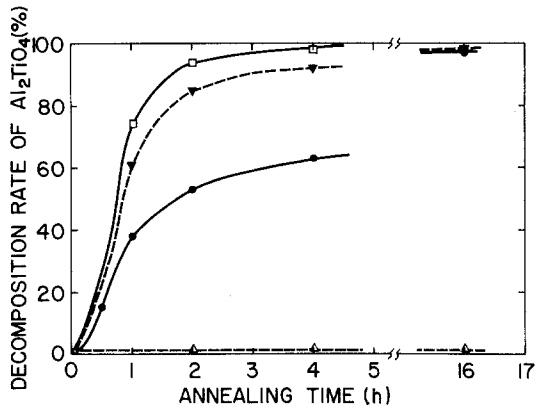

Figure 20 Decomposition rate of Al_2TiO_5 phase for sintered and annealed Al_2O_3–TiO_2 compacts having different TiO_2 contents (mol %): (●) 20, (△) 30, (□) 40, (▼) 60, (——) with cooling process, (– – –) without cooling process.

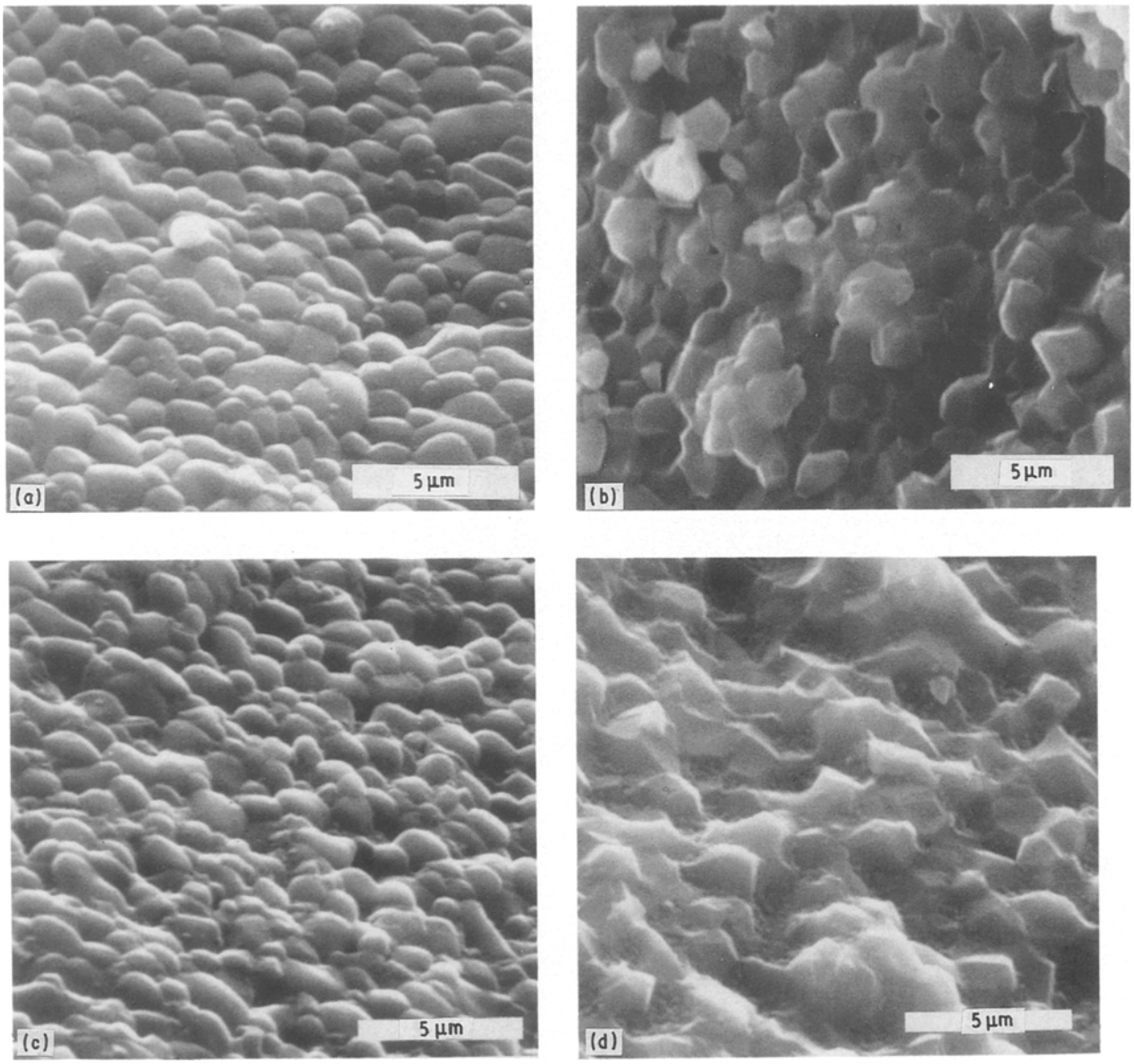

Figure 21 Scanning electron micrographs of: (a) top surface, and (b) fracture surface of Al_2O_3–20 mol % TiO_2 powder compact fired at 1500° C for 1.5 h; (c) top surface and (d) fracture surface of the same compact cooled to 200° C then annealed at 1200° C for 16 h.

The time period at peak temperature required to achieve a high density depended on the green density of the compact prepared by filter casting. Compacts containing 10 mol % TiO_2 (bulk density 50% to 55%) and fired at 1500° C reached a density of 98% theoretical in 30 min (Fig. 15). Compacts containing 20 mol % TiO_2 (bulk density 45% to 50%) reached a density of 95% theoretical when fired at 1500° C for 30 min (Fig. 16). Green compacts having lower bulk densities needed longer firing periods; compacts containing 30 mol % TiO_2 (35% to 40% bulk density) took 5 h at 1500° C to reach a density of 95% theoretical (Fig. 17). Compacts containing 60 mol % TiO_2 (35% bulk density) took 5 h at 1500° C to reach a density of 90% theoretical (Fig. 18). These results demonstrate the importance of the density and packing conditions of the green body.

X-ray diffraction analysis of the fired compacts indicated that compacts with TiO_2 contents of less than 50 mol % became two-phase structures of Al_2TiO_5 and Al_2O_3; compacts containing 60 mol % TiO_2 resulted in a two-phase structure of rutile and Al_2TiO_5. The difference in grain growth between compacts with less than 50 mol % TiO_2 and those with 60 mol % TiO_2 can be explained by the resulting compacts' crystal structure; excess Al_2O_3 is effective toward reducing the grain growth of Al_2TiO_5 [10].

Chemical compositions for the sintered compacts analysed by electron probe microanalysis are summarized in Table III. Analysis results agreed well with the results of quantitative X-ray diffraction analysis for composite powders.

TABLE III Chemical compositions for sintered Al_2O_3–TiO_2 specimens with different TiO_2 contents

TiO_2 content (mol %)	Calculated composition (wt %)		Measured composition* (wt %)	
	TiO_2	Al_2O_3	TiO_2	Al_2O_3
10	8.01	91.99	6.06	91.80
20	16.38	83.62	16.88	81.98
50	43.93	56.07	42.33	56.13
60	54.03	45.97	52.50	47.52

*Measured by electron probe microanalysis.

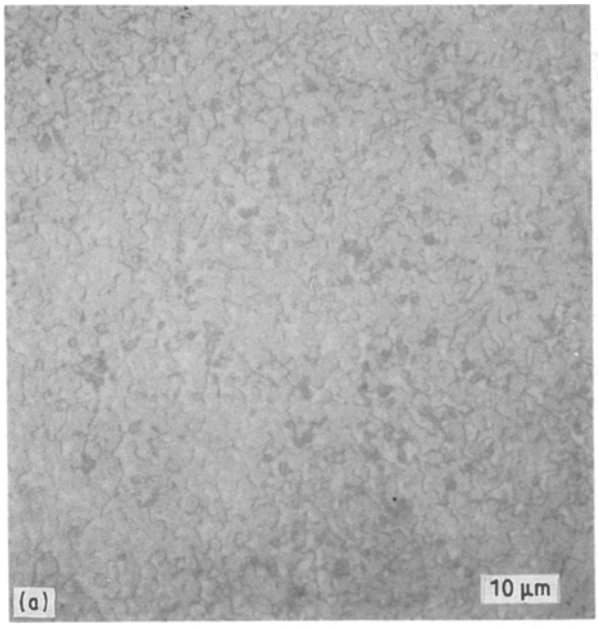

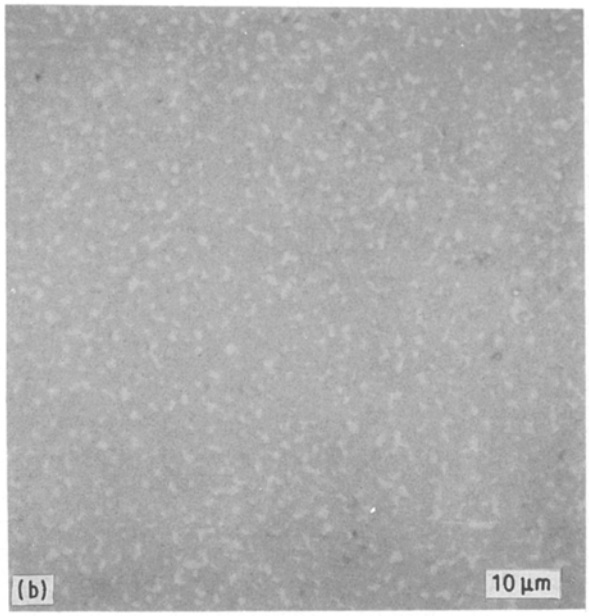

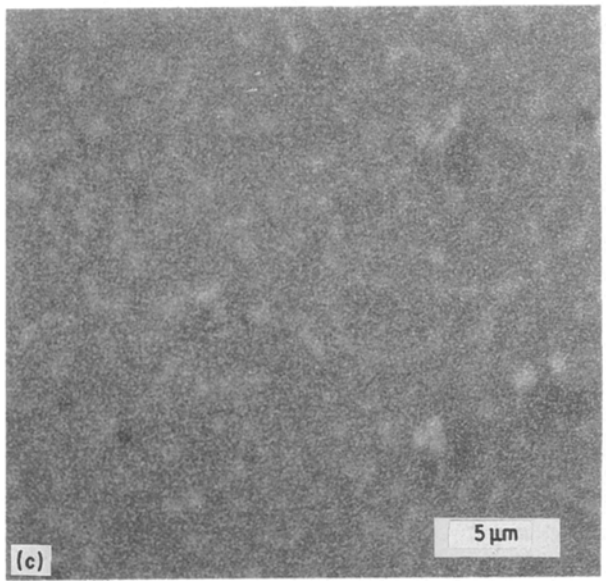

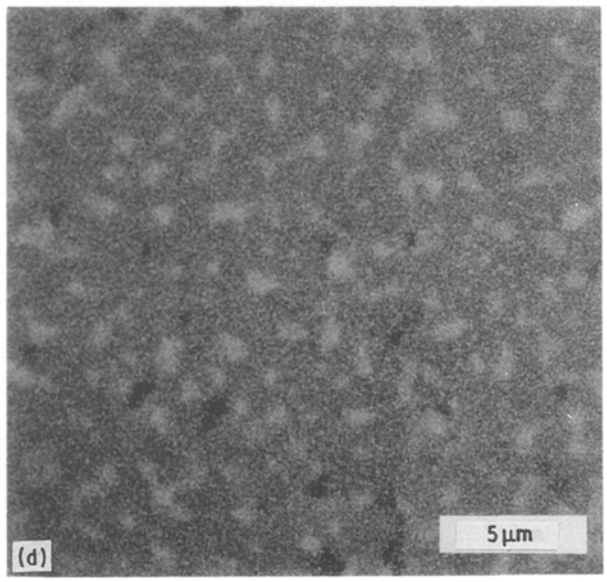

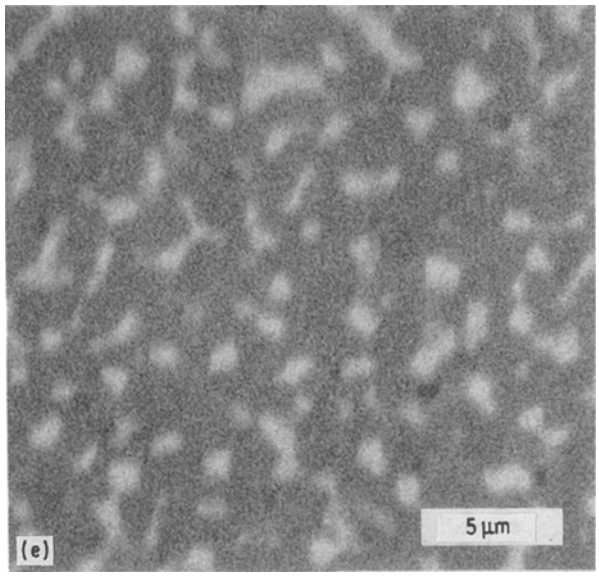

Figure 22 Optical micrographs of: (a) polished surface of an Al_2O_3–20 mol % TiO_2 compact fired at 1500° C for 1.5 h, and (b) polished surface of the same compact after annealing at 1200° C for 16 h (with cooling process to 200° C after sintering); scanning electron micrographs (backscattering image) of: (c) polished surface of an Al_2O_3–20 mol % TiO_2 compact fired at 1500° C for 1.5 h, cooled to 200° C, and annealed at 1200° C for 30 min, (d) same surface annealed for 2 h, and (e) same surface annealed an additional 14 h (total 16 h).

Specimens containing 50 mol % TiO_2 and fired at 1350° C for 5 h had different microstructures when polished and chemically etched than did similar specimens fired at 1280° C for 20 h (Fig. 19). The specimens fired at 1350° C had a finer microstructure; a fine TiO_2 network indicates an Al_2TiO_5 crystal structure (Figs 19a, b). Specimens fired at 1280° C had a composite structure; TiO_2 crystals ran irregularly through the body (Figs 19c, d). The latter structure is desirable for strong ceramic composite bodies. However, high density cannot be expected for the specimens sintered below 1300° C. Therefore, an annealing treatment, as described below, was performed for the high-density specimen fired above 1300° C to achieve the desired microstructure.

It is known that the Al_2TiO_5 crystal phase is unstable at temperatures below 1300° C and decomposes to the binary phase of rutile and Al_2O_3 [11, 12].

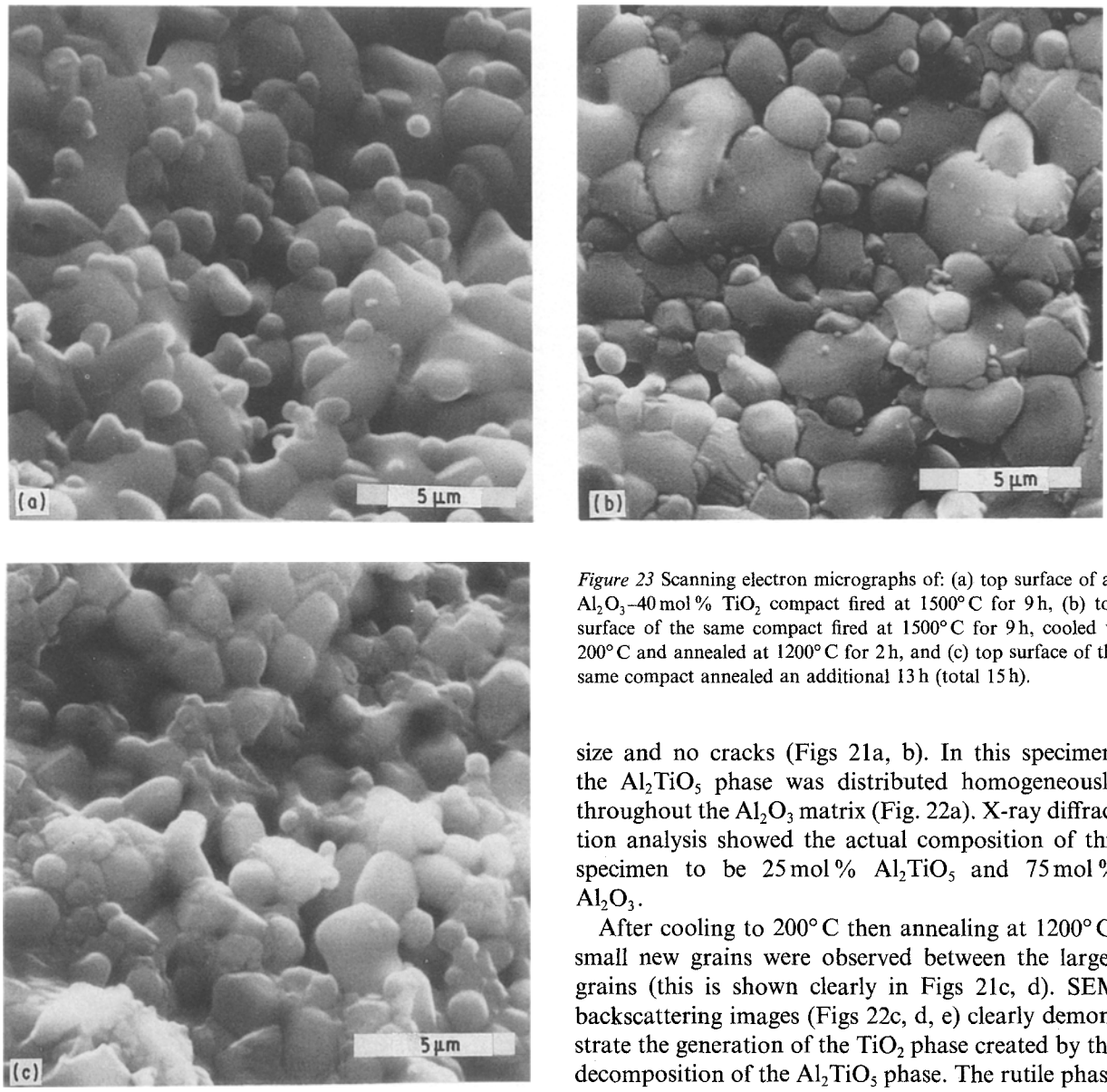

Figure 23 Scanning electron micrographs of: (a) top surface of an Al_2O_3–40 mol % TiO_2 compact fired at 1500° C for 9 h, (b) top surface of the same compact fired at 1500° C for 9 h, cooled to 200° C and annealed at 1200° C for 2 h, and (c) top surface of the same compact annealed an additional 13 h (total 15 h).

The decomposition of Al_2TiO_5 is thought to be controlled by nucleation and growth [13]. Annealing results for the sintered specimens (Fig. 20) confirmed that nucleation rather than growth plays an important role in the decomposition process. Specimens having excess TiO_2 with Al_2TiO_5 (60 mol % TiO_2) completely decomposed to TiO_2 (rutile) and Al_2O_3 within 16 h by annealing at 1200° C after sintering at 1500° C. On the other hand, specimens having excess Al_2O_3 with Al_2TiO_5 (10, 20, 30 and 40 mol % TiO_2) did not decompose by annealing at 1200° C after sintering at 1500° C. However, the same specimens decomposed to rutile and Al_2O_3 when cooled to 200° C and then annealed at 1200° C after sintering at 1500° C within 5 to 16 h. (When cooled directly to the annealing temperature, the Al_2TiO_5 phase decomposition was so slow that rutile was not detected even after annealing for 16 h.)

The microstructure of the specimen before, during, and after annealing was observed by SEM and optical microscopy. Figs 21 and 22 illustrate the typical microstructural change due to the decomposition of Al_2TiO_5 to TiO_2 and Al_2O_3. The 20 mol % TiO_2 specimen sintered at 1500° C for 1.5 h had a small grain size and no cracks (Figs 21a, b). In this specimen, the Al_2TiO_5 phase was distributed homogeneously throughout the Al_2O_3 matrix (Fig. 22a). X-ray diffraction analysis showed the actual composition of this specimen to be 25 mol % Al_2TiO_5 and 75 mol % Al_2O_3.

After cooling to 200° C then annealing at 1200° C, small new grains were observed between the larger grains (this is shown clearly in Figs 21c, d). SEM backscattering images (Figs 22c, d, e) clearly demonstrate the generation of the TiO_2 phase created by the decomposition of the Al_2TiO_5 phase. The rutile phase structure created by the decomposition of Al_2TiO_5 was composed of fine grains homogeneously distributed throughout the Al_2O_3 grain matrix (Fig. 22b).

A similar change in the microstructure was observed for other specimens, as shown in Fig. 23 (40 mol % TiO_2, after sintering: 67 mol % Al_2TiO_5) and Fig. 24 (60 mol % TiO_2, after sintering: 67 mol % Al_2TiO_5 and 33 mol % TiO_2). Figs 24a and b show that excess TiO_2 appeared as individual grains in the Al_2TiO_5 matrix. This specimen easily decomposed to rutile and Al_2O_3 during a 4 h annealing period when cooled to the annealing temperature. Annealing and the consequent decomposition resulted in a predominant rutile phase and a highly branched TiO_2 matrix (Fig. 24c).

Fracture toughness (K_{Ic}) for the fired, and fired and annealed specimens was measured using the micro-Vicker's indentation test and calculated using Niihara's equation [14]. Results are given in Fig. 25. Vicker's hardness values (H_v) are given in Fig. 26. Specimens having relatively lower TiO_2 contents (e.g. 20 and 30 mol % TiO_2) showed high H_v values and relatively high K_{Ic} values, which were improved by annealing. On the other hand, specimens having higher TiO_2 contents (e.g. 40, 50 and 60 mol % TiO_2) showed low H_v values. The K_{Ic} values for these specimens were difficult to measure due to already existing

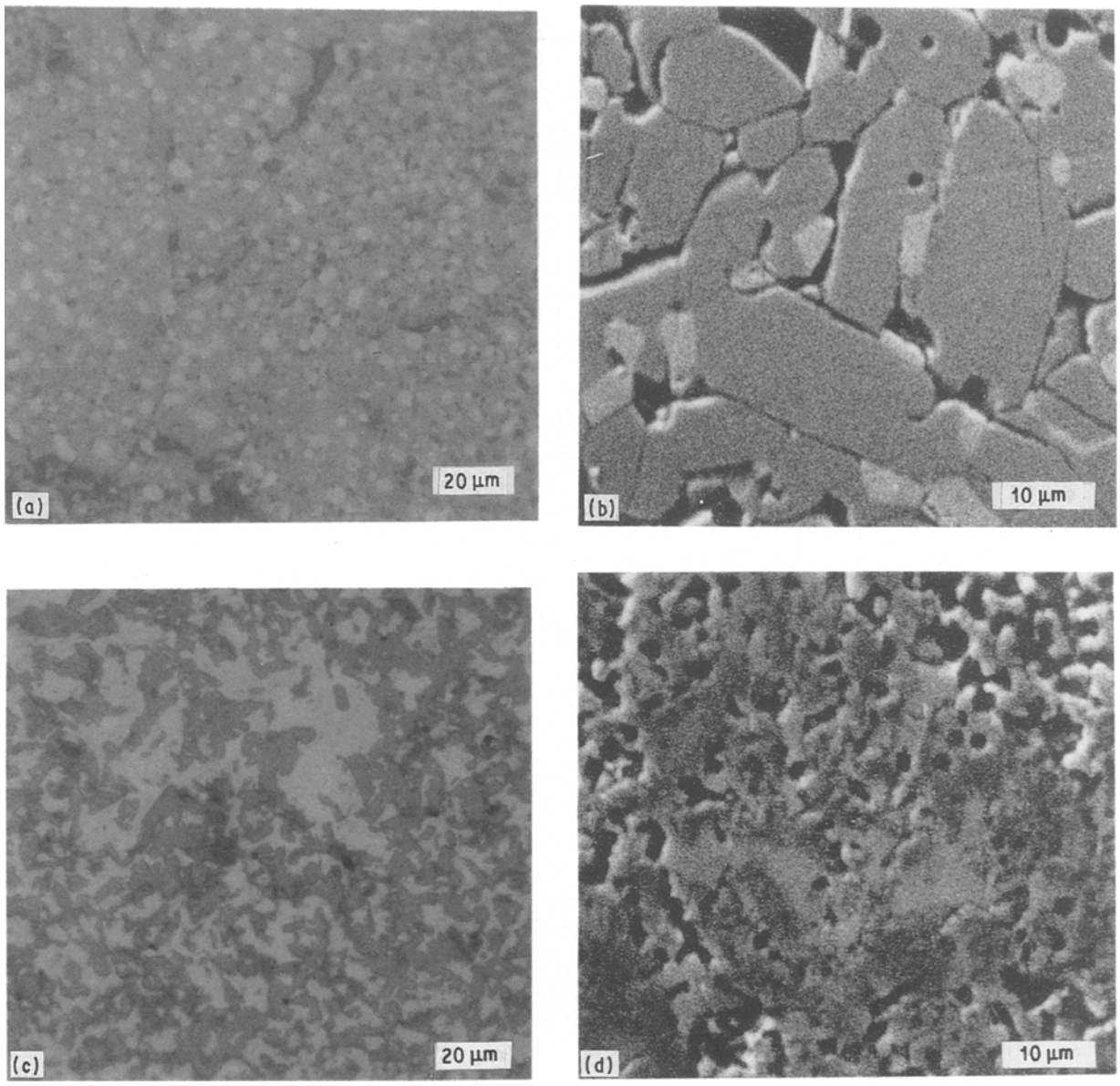

Figure 24 (a) Optical micrograph of a polished surface of an Al_2O_3–60 mol % TiO_2 compact fired at 1500° C for 5 h, (b) scanning electron micrograph (backscattering image) of the same compact, (c) optical micrograph of the same compact after annealing at 1200° C for 15 h, and (d) scanning electron micrograph (backscattering image) of compact (c).

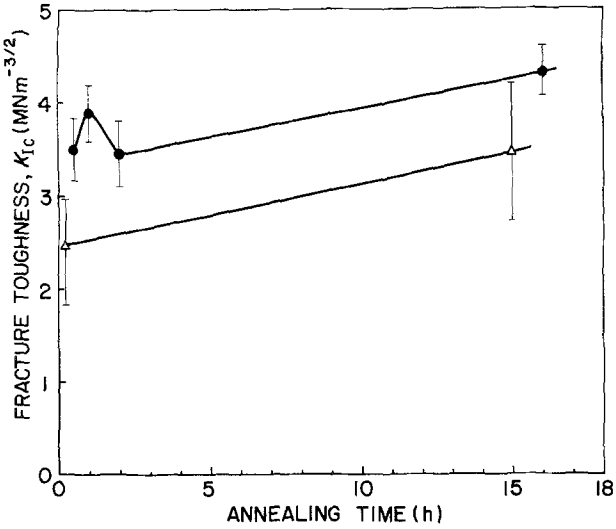

Figure 25 Fracture toughness (K_{1c}) for Al_2O_3–TiO_2 compacts containing (●) 20 and (△) 30 mol % TiO_2 and fired at 1500° C for 1.5 h then annealed (with cooling process after sintering).

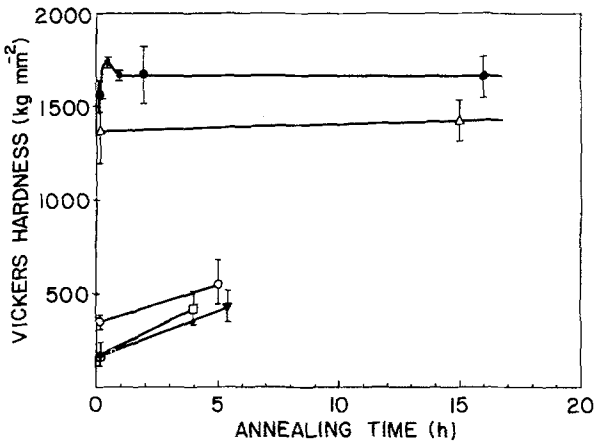

Figure 26 Vicker's hardness for Al_2O_3–TiO_2 composite powder compacts containing 20 to 60 mol % TiO_2, fired at 1500° C for 1.5 h, and fired and annealed at 1200° C (with cooling process for the 20 to 50 mol % TiO_2 compacts and without cooling for the 60 mol % TiO_2 compact). TiO_2 (mol %): (●) 20, (△) 30, (□) 40, (○) 50, (▼) 60.

cracks (domain-boundary cracks or grain-boundary cracks).

4. Conclusions

1. Al_2O_3–TiO_2 composite powders having a narrow size distribution and a desirable TiO_2 content were reproducibly prepared by the stepwise hydrolysis of titanium alkoxide in an Al_2O_3 dispersion.

2. Particle size and TiO_2 content of the composite powders were controlled by selecting the particle size of the starting Al_2O_3 powder and the amount of alkoxide hydrolysed.

3. Al_2TiO_5 composite specimens of high density (95% to 98% theoretical) were obtained from the green compacts of the Al_2O_3–TiO_2 composite powders by firing at a temperature above 1300° C.

4. Microstructure, physical properties, and crystal phase of the fired specimens were controlled by selecting firing and annealing conditions.

Acknowledgement

The support of the MIT-Industry Ceramics Processing Research Consortium is gratefully acknowledged.

References

1. H. K. BOWEN, *Mater. Sci. Engng* **44** (1980) 1.
2. G. Y. ONODA Jr and L. L. HENCH, "Ceramic Processing before Firing" (Wiley, New York, 1978).
3. E. A. BARRINGER and H. K. BOWEN, *J. Amer. Ceram. Soc.* **65** (1982) C-199.
4. B. FEGLEY Jr, E. A. BARRINGER and H. K. BOWEN, *ibid.* **67** (1984) C-113.
5. B. FEGLEY Jr and E. A. BARRINGER, in "Better Ceramics through Chemistry", edited by C. J. Brinker (Elsevier, New York, 1984) p. 187.
6. B. NOVICH, Ceramics Processing Research Laboratory Report no. M1, Massachusetts Institute of Technology (1984).
7. R. H. HEISTAND, II, Y. OGURI, H. OKAMURA, W. C. MOFFATT, B. NOVICH, E. A. BARRINGER and H. K. BOWEN, in "Science of Ceramic Processing", edited by L. L. Hench and D. R. Ulrich (John Wiley & Sons, New York, 1985) p. 482.
8. H. OKAMURA, E. A. BARRINGER and J. K. BOWEN, *J. Amer. Ceram. Soc. Comm.* **69** (1986) C-22.
9. A. M. LEJUS, D. GOLDBERG and A. REVCOLEVASCHI, *C.R. Acad. Sci.* **263** (1966) 1223.
10. Y. OHYA, K. HAMANO and Z. NAKAGAWA, *J. Ceram. Soc. Jpn* **91** (1983) 289.
11. S. M. LANG, C. L. FILLMORE and L. M. MAXWELL, *J. Res. Nat. Bur. Std.* **48** (1952) 298.
12. A. M. LEJUS, D. GOLDBERG and A. REVCOLEVASCHI, *Comt. Rend. Acad. Sci.* **C263** (1966) 1223.
13. T. KAMEYAMA and T. YAMAGUCHI, *J. Ceram. Soc. Jpn* **84** (1976) 589.
14. K. NIIHARA, *J. Mater. Sci. Lett.* **2** (1983) 221.
15. H. OKAMURA, E. BARRINGER and H. K. BOWEN, *J. Amer. Ceram. Soc. Comm.* **69** [2] C-22-C-24 (February 1986), © 1986. Taken from "Preparation and Sintering of Monosized Al_2O_3–TiO_2 Composite Powder".

Received 25 March
and accepted 29 July 1988